F.O. ADURODIJA[1],✉
R. BRÜNING[1]
I.O. ASIA[2]
H. IZUMI[3]
T. ISHIHARA[3]
H. YOSHIOKA[3]

# Effects of laser irradiation energy density on the properties of pulsed laser deposited ITO thin films

[1] Physics Department, Mount Allison University, 67 York Street, Sackville, N.B., E4L 1E6, Canada
[2] Chemistry Department, Ambrose Alli University, Ekpoma, Nigeria
[3] Hyogo Prefectural Institute of Industrial Research, 3-1-12 Yukihira-cho, Suma-ku, Kobe 654-0037, Japan

**ABSTRACT** The properties of indium tin oxide (ITO) thin films, deposited at room temperature by simultaneous pulsed laser deposition (PLD), and laser irradiation of the substrate are reported. The films were fabricated from different Sn-doped $In_2O_3$ pellets at an oxygen pressure of 10 mTorr. During growth, a laser beam with an energy density of 0, 40 or 70 mJ/cm$^2$ was directed at the middle part of the substrate, covering an area of $\sim 1$ cm$^2$. The non-irradiated (0 mJ/cm$^2$) films were amorphous; films irradiated with 40 mJ/cm$^2$ exhibited microcrystalline phases; and polycrystalline ITO films with a strong $\langle 111 \rangle >$ preferred orientation was obtained for a laser irradiation density of 70 mJ/cm$^2$. The resistivity, carrier density, and Hall mobility of the ITO films were strongly dependent on the Sn doping concentration and the laser irradiation energy density. The smallest resistivity of $\sim 1 \times 10^{-4}$ $\Omega$ cm was achieved for a 5 wt % Sn doped ITO films grown with a substrate irradiation energy density of 70 mJ/cm$^2$. The carrier mobility diminished with increasing Sn doping concentration. Theoretical models show that the decrease in mobility with increasing Sn concentration is due to the scattering of electrons in the films by ionized centers.

**PACS** 81.15.Fg; 73.61.-r; 73.50.-h

## 1 Introduction

Indium tin oxide (ITO) has been studied for many years [1, 2]. It is found in many applications such as flat panel displays [3], liquid crystal displays [5], solar cells [1, 2], organic light emitting devices [5], and electrochromic devices [6]. Its numerous applications are due to low resistivity and high transmission of the visible light, high near-infrared reflectance [2], excellent substrate adherence, hardness, and chemical inertness [1, 2]. In some applications, such as organic light emitting devices, tolerance for substrate heating is very low. Hence, a low deposition temperature of less than 200 °C is required for the ITO films. It is well known that ITO films deposited at room temperature are amorphous or, at best, nano- or microcrystalline [7]. Fully polycrystalline films are only achieved at substrate temperature above 200 °C. Present

research efforts have been directed at developing techniques for producing low resistivity ITO films on unheated or heated substrates ($\leq 100$ °C). This is driven by industries that require the use of heat sensitive substrates such as polycarbonates for device applications [8].

Low-resistivity and high optical transmittance ITO thin films have been produced by a variety of techniques, sputtering [1, 2], chemical vapor deposition [9], electron beam evaporation [2], spray pyrolysis [1], sol gel [10], and PLD [11]. However, because the electro-optical properties of the films are subject to the deposition conditions, each technique has produced films with different properties. At low temperature, PLD has produced ITO films with the best, compared to other techniques, electro-optical and microstructural properties.

In this paper we report the electrical and structural properties of ITO films deposited at room temperature by simultaneous PLD and laser irradiation of the substrate. Laser beams of different irradiation energy density were used to deposit ITO films with 0 wt % to 10 wt % tin (Sn) doping concentrations on fused silica glass substrates. The electronic conduction mechanisms are also explained.

## 2 Experimental

ITO films were deposited using a KrF (248 nm) excimer laser (Lambda Physik, COMPex 102) system. Details on the experimental setup have been reported elsewhere [8, 11]. Prior to film deposition the deposition chamber was pumped down to a pressure of $10^{-6}$ Torr using a turbomolecular pump. Five 2 cm diameter targets, arranged in a circular form, were mounted on a holder. The laser beam was focused on the target surface through a quartz glass window using a bi-convex lens. The distance between the target and the substrate was 7 cm.

The laser beam, with a total energy of 300 mJ operating at frequency of 20 Hz, was split into two parts using a beam splitter. One part of the beam was focused on the target and the second part was directed onto the centre of the substrate surface using a plano convex lens. The laser irradiation beam incident on the target produced an energy density of 5 J/cm$^2$. The laser irradiation beam incident on the substrate had energy densities of 0, 40 and 70 mJ/cm$^2$. Higher energy density led to re-evaporation of the growing ITO films. At 0 mJ/cm$^2$ laser beam was shuttered. Hot-pressed sintered ceramic tar-

✉ Fax: +1-506-364-2583, E-mail: oadurodi@mta.ca

gets consisting of 99.99% pure undoped $In_2O_3$ (0 wt % Sn) and Sn-doped (3, 5 and 10 wt %) $In_2O_3$ were used. The films were deposited on $SiO_2$ glass substrates at room temperature at a fixed oxygen pressure of 10 mTorr. At these conditions, a deposition rate of 12 nm/min was achieved as indicated by a vibrating quartz microbalance located near the substrate.

The film thickness of the ITO films, $100 \pm 20$ nm, was measured by a stylus surface profilometer (Dektak 3ST). X-ray diffraction spectra of the films were obtained with a Rigaku: Rint-2000 diffractometer using a Cu $K_\alpha$ ($\lambda = 1.5405$ Å) radiation. The electrical properties of the films were examined by the Hall measurements.

## 3 Results and discussion

### 3.1 *Structural properties*

Typical XRD spectra of ITO films laser irradiated with energy densities of 0, 40, and 70 mJ/$cm^2$ during the room temperature PLD are shown in Fig. 1. With increasing laser energy density, the ITO film changed from amorphous to the crystalline phase. The non-irradiated (0 mJ/$cm^2$) films were amorphous as indicated by the absence of diffraction peaks, Fig. 1(a). Increasing the laser irradiation energy density to 40 mJ/$cm^2$ produced a partially crystalline phase as indicated by the emergence of a small (222) peak, Fig. 1(b). Further increase of the laser irradiation energy density to 70 mJ/$cm^2$ yielded fully polycrystalline ITO films with a strong $\langle 111 \rangle$ preferred orientation, Fig. 1(c). Raising the laser irradiation energy density to 100 mJ/$cm^2$ resulted in the re-ablation of the already deposited films.

Ultraviolet photon energy excitation of the film surface, and dissociation of the gas phase during PLD growth process have been shown to improve the morphology, crystallinity, and preferred orientation of superconducting, ferroelectric, and transparent conducting oxide thin films [12–14]. This ef-

fect resulted from the nonequilibrium heating which enabled the heating of only the surface of the film. With substrate laser irradiation, the enhancement in the crystalline structure of the ITO films is attributed to an increased surface mobility of the adatoms due to photochemical and photothermal effects. The increased adatoms surface mobility creates nucleation sites and annealing of surface defects with a consequential improvement in the crystalline features. It is also anticipated that in the presence of oxygen gas, laser irradiation could lead to selective excitation and photo-dissociation of the plasma in the proximity of the substrate, hence producing excited precursor atoms for the film growth. Therefore, at room temperature laser irradiation of the substrates during film growth facilitates the reaction via photo-induced excitation and enhanced mobility of the chemical species in the plasma.

### 3.2 *Electrical properties*

The electrical properties of ITO films irradiated with different energy densities as a function of Sn doping levels are shown in Fig. 2. The resistivity for the non-irradiated films and films irradiated with 40 mJ/$cm^2$ are similar, and the resistivity increases moderately with Sn doping levels as shown in Fig. 2(a). These films were amorphous as observed from the XRD data, as discussed above. A resistivity value as low as $\sim 2 \times 10^{-4}$ $\Omega$ cm was obtained for an undoped $In_2O_3$ (0 wt % Sn) film irradiated with a 40 mJ/$cm^2$ laser beam. In contrast, undoped $In_2O_3$ films irradiated with laser beam of energy density of 70 mJ/$cm^2$ showed a high resistivity of $\sim 4 \times 10^{-4}$ $\Omega$ cm. This high resistivity presumably resulted from a decrease in the oxygen vacancies during crystallization of the film [15, 16]. The resistivity dropped to $1.2 \times 10^{-4}$ $\Omega$ cm as the Sn doping concentration was raised to 3 wt %. The resistivity remains low over the Sn doping con-
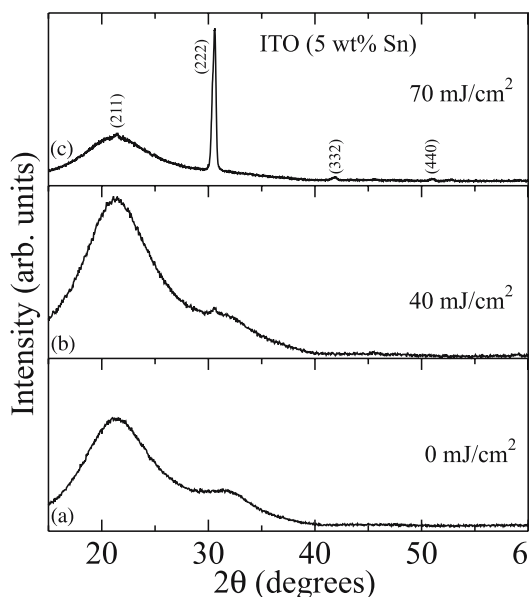


**FIGURE 1** XRD spectra of ITO films deposited at oxygen pressure of 10 mTorr and irradiation energy density of (a) 0 mJ/$cm^2$ (non-irradiated), (b) 40 mJ/$cm^2$, and (c) 70 mJ/$cm^2$
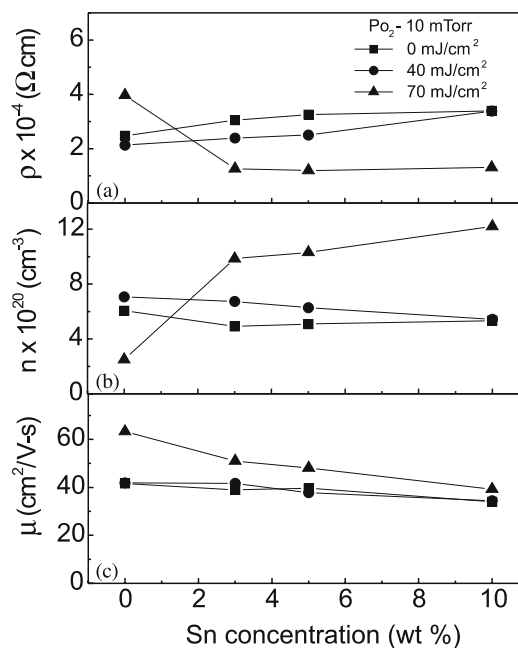


**FIGURE 2** Plots of (a) resistivity ($\varrho$), (b) carrier density ($n$) and (c) Hall mobility ($\mu$) against Sn doping concentration for films irradiated with energy density of (a) 0 mJ/$cm^2$, (b) 40 mJ/$cm^2$, and (c) 70 mJ/$cm^2$

centration range of 3 to 10 wt % investigated. However, the film containing 10 wt% Sn showed a slightly higher resistivity of $1.5 \times 10^{-4}$ $\Omega$ cm compared to the (3 and 5) wt % Sn doped ITO films and this increase could be related to increasing presence of impurity scattering centers [16–19]. The lowest resistivity of $1.1 \times 10^{-4}$ $\Omega$ cm was measured for a 5 wt % Sn-doped ITO film.

Figure 2(b) shows the carrier density of the ITO films. The non-irradiated and the films irradiated with an energy density of 40 mJ/cm$^2$ yielded stable carrier density of $(5 - 7) \times 10^{20}$ cm$^{-3}$ for all doping levels. This indicates that Sn doping contributes few conduction electrons in the amorphous or microcrystalline ITO films. Actually, a slight decrease of carrier density with Sn doping agrees with findings reported in the literature [11, 18, 19]. In contrast, the carrier density of the crystalline films irradiated at 70 mJ/cm$^2$ depends strongly on the doping level, Fig. 2(a). In the case of the undoped In$_2$O$_3$ films, a low carrier density of $\sim 2.5 \times 10^{20}$ cm$^{-3}$ was measured. The carrier density increased to $9.8 \times 10^{20}$ cm$^{-3}$ with an increase in the Sn doping concentration to 3 wt %. A further rise in the Sn doping concentration to 10 wt % produced an additional increase in the carrier density to $1.2 \times 10^{21}$ cm$^{-3}$.

In a polycrystalline ITO film, an Sn atom with four valence electrons replaces an indium atom with three valence electrons in the crystal lattice, thereby giving an extra electron to the conduction band. In addition to Sn doping effect, carriers are contributed to the ITO films by doubly charged oxygen vacancies. In the amorphous phase, evidence suggests that Sn atoms do not supply effective carriers; rather carriers are generated mainly by the creation of oxygen vacancies [20]. The observed flatness of the carrier density versus Sn doping concentration also confirms this assumption.

In Fig. 2(c) a similarity in the plots of the Hall mobility against the Sn doping concentration for the non-irradiated and the 40 mJ/cm$^2$ laser irradiated ITO films is noticed. The Hall mobility decreased from (42 to 35) cm$^2$/Vs with increasing Sn doping concentration. In the case of the films irradiated with energy density of 70 mJ/cm$^2$, undoped In$_2$O$_3$ film produced a high Hall mobility of 63.3 cm$^2$/Vs and the value decreased gradually to 42.5 cm$^2$/Vs with an increase in the Sn doping concentration to 10 wt %. A decrease in the Hall mobility is observed for all the films as the amount of Sn included in the films increases irrespective of their crystalline phase. A similar dependence of the Hall mobility on the Sn doping concentration was reported for ITO thin films deposited by electron-beam-evaporation and PLD and the effect is attributed to the presence of complexes that acts as scattering centers [16, 18, 19]. However, compared to the amorphous films, the higher mobility attained in the ITO films irradiated with energy density 70 mJ/cm$^2$ is due to the improvements in the crystalline structure. The moderately low mobility obtained at high Sn-doping concentration may be due to the interaction of scattering centers and formation of neutral scattering defect [11, 16–19].

### 3.3 *Electronic conduction mechanisms*

The Hall mobility of ITO films is affected by the disorder of the In$_2$O$_3$ structure and a change of the network resulting from Sn doping [16–19]. As the Sn doping concen-

tration increases, complexes form which do not supply conducting free electrons, but only act as scattering centers that lower the mobility of free electrons [16, 17, 21]. Electron scattering sources such as grain boundaries, acoustical phonons, neutral and ionized impurity centers affect the electrical and optical properties of ITO films [17]. However, many of the cases that have been examined show that grain boundaries and acoustical phonons play minor roles because the mean free path of the electron is smaller than the average crystallite size. Therefore, the electrical transport properties do not change significantly with temperature [17, 22].

The experimental data of the non-irradiated and laser-irradiated ITO films were studied further to explain the dominant scattering process. Hence, the mean free path, $l$, was calculated using a sufficiently degenerate gas model, given by [16, 17, 23]

$$l = V_f\tau = (3\pi^2)^{1/3}(\hbar/e^2)\varrho^{-1}n^{2/3} \qquad (1)$$

where

$$V_f = (3\pi^2)^{1/3}(\hbar/m^*)n^{1/3} \qquad (2)$$

is the electron velocity at the Fermi surface.

Here $m^*$ and $n$ denote the electron velocity at the Fermi surface, electron effective mass and carrier density, respectively. The relaxation time and the resistivity are represented by $\tau$ and $\varrho$. Within the boundaries of experimental error ($\sim 2\%$), the calculated mean free paths plotted against Sn doping concentration are shown in Fig. 3. No obvious change in the mean free paths ($l < 11$ nm) of the amorphous or microcrystalline films ($l \sim 7.5$ nm) and the polycrystalline ITO films occurred. The calculated $l$ was a lot smaller than the average crystallite sizes of about 200 nm observed from the AFM measurements (not shown here). Therefore, it is summarized that contribution of electron scattering at grain boundaries is trivial.

In most of the cases reported in the literature, the scattering of the conduction electrons in the ITO films by neutral and ionized impurity centers seemed to be common [17, 18]. Erginsoy calculated the contribution to conductivity due to neutral impurities for semiconductors with small degrees of
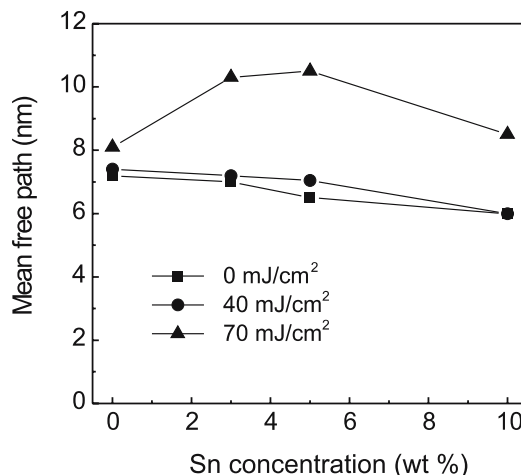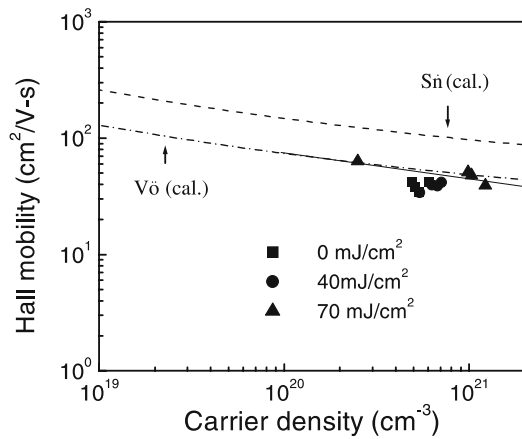


**FIGURE 3** Plots of the mean free paths versus Sn doping concentration

**FIGURE 4** Hall mobility versus carrier density for ITO films irradiated with different energy densities: showing experimental data and calculated mobilities based on scattering by ionized impurities and the assumption that all the carriers are due to singly charged tin (Sṅ) donors or doubly charged oxygen vacancies (Vö)

ionization [24]. Conwell and Weisskopf [25], and Dingle [26] provided a theoretical assessment of the contribution to conductivity of ITO film due to ionized scattering. The above named theories, given below, were used to further explain the electronic transport mechanisms. Others researchers have studied the effect of neutral and charge scattering centers on the mobility in degenerate semiconductors based on the above theories [16, 18, 27–29].

The total mobility $\mu_T$ is given as the sum of $\mu_N$ and $\mu_I$ as follows:

$$\frac{1}{\mu_T} = \frac{1}{\mu_N} + \frac{1}{\mu_I} \tag{3}$$

where

$$\mu_N = \frac{(m^* e^3)}{20 \varepsilon_o \varepsilon_r \hbar^3 n_N} \tag{4}$$

and

$$\mu_I = \frac{24 \pi^3 (\varepsilon_o \varepsilon_r)^2 \hbar^3 n}{e^3 m^{*2} g(x) Z^2 n_I} . \tag{5}$$

The screening function $g(x)$ is given by

$$g(x) = \ln\left(1 + \frac{4}{x}\right) - \left(1 + \frac{4}{x}\right)^{-1} \tag{6}$$

where

$$x = \frac{4 e^2 m^*}{4 \pi \varepsilon_o \varepsilon_r \hbar^2 (3\pi^5)^{1/3} n^{1/3}} \tag{7}$$

$\mu_N$ and $\mu_I$ signify the mobilities due to neutral and charged centers, respectively. $\varepsilon_o$ is the permittivity of free space. $m^*$ and $\varepsilon_r$ are the effective mass of the electron and low-frequency of permittivity. In the case of ITO films the values of $m^*$ and $\varepsilon_r$ are taken as $0.3 m_e$ [16, 26] and 9 [2, 16], respectively. $n$ and $Z$ denote the carrier density and the charge of the ionized centers, respectively. $n_N$ and $n_I$ denote neutral and ionized scattering centers, respectively.

It is generally known that in polycrystalline ITO films, free electron donors originating from substitutional four-valence Sn atoms (i.e., supply of one electron or Sn) and oxygen vacancies (supply of two electrons or Vö) control the behaviors of the electronic properties. Essentially, the scattering caused by doubly charged oxygen vacancies (Vö) is greater than that of the single charge from Sn (Sṅ), because the values of $n/n_I Z^2$ (from (5)) (Vö) and (Sṅ) are 1 and 0.5, respectively [16]. Plots of the measured Hall mobility versus carrier density for the ITO films are shown in Fig. 4. Using (5), the calculated $\mu_I$ plotted as a function of $n$ assuming that the measured mobility was entirely due to either charged vacancies (Vö) or singly charged Sn (Sṅ) is also shown in Fig. 4. A good agreement was obtained between the gradients of the measured and the calculated mobilities against the carrier densities. Therefore, it was concluded that scattering at ionized centers could account for the decrease in the Hall mobility of the ITO films. However, since the increase in carrier density was largely associated with the increase in Sn doping concentration, Fig. 2(a), the presence of some Sn atoms may also act as neutral scattering centers.

## 4    Conclusion

The properties of ITO thin films deposited on glass substrates at room temperature by simultaneous PLD and laser irradiation during growths have been discussed. The effects of a laser beam with energy densities of 0, 40 and 70 mJ/cm$^2$ on the structural and electrical properties of the ITO films with Sn doing concentrations varying from $(0 - 10)$ wt% were examined. By increasing the energy of the laser irradiation beam focused onto the substrate during growths (up to 70 mJ/cm$^2$), polycrystalline ITO films with a strong $\langle 111 \rangle$ preferred orientation were produced. ITO films with low resistivities of $\sim 2 \times 10^{-4}$ and $\sim 1 \times 10^{-4}$ $\Omega$ cm were achieved for 0 wt % (undoped In$_2$O$_3$) and 5 wt % Sn-doped ITO films at laser densities of 40 and 70 mJ/cm$^2$, respectively. Studies of the electron conduction mechanisms indicated that scattering of free carriers in the films was mainly caused by ionized centers.

### REFERENCES

1 K.L. Chopra, S. Major, D.K. Pandya: Thin Solid Films **102**, 102 (1983)
2 I. Hamberg, C.G. Granqvist: J. Appl. Phys. **60**, R123 (1986)
3 B.H. Lee, I.G. Kim, S.W. Cho, S.H. Lee: Thin Solid Films **302**, 25 (1977)
4 N.D. Young, R.M. Bunn, R.W. Wilks, D.J. McCulloch, S.C. Deane, M.J. Edwards, G. Harkin, A.D. Pearson: J. Soc. Inf. Disp. **5/3**, 275 (1997)
5 G. Gustafon, Y. Cao, G.M. Treacy, F. Klavetter, N. Colaneri, A.J. Heeger: Nature (London) **357**, 477 (1992)
6 C.G. Granqvist: Adv. Mater. **15**, 1789 (2003)
7 Y. Shigesato, R. Koshi-ishi, T. Kawashima, J. Ohsako: Vacuum **59**, 614 (2000)
8 H. Izumi, T. Ishihara, H. Yoshioka, M. Motoyama: Thin Solid Films **411**, 32 (2002)
9 T. Maruyama, K. Fukui: J. Appl. Phys. **70**, 3848 (1991)
10 M.J. Alam, D.C. Cameron: Surf. Coat. Technol. **142**, 776 (2001)
11 F.O. Adurodija: *Handbook of Thin Films: Deposition and Processing of Films*, H.S. Nalwa (Ed.), Vol. 1 (Academic Press, New York 2001) p. 161
12 H. Hosono, M. Kurita, H. Kawazoe: Jpn. J. Appl. Phys. **37**, L1119 (1998)
13 H. Tabata, O. Murata, T. Kawai, S. Kawai, M. Okuyama: Jpn. J. Appl. Phys. **31**, L2968 (1998)

14 S. Otsubo, T. Minamikawa, Y. Yonezawa, A. Morimoto, T. Shimizu: Jpn. J. Appl. Phys. **29**, L73 (1990)
15 H. Kim, C.M. Gilmore, A. Pique, J.S. Horwitz, H. Mattoussi, H. Murata, Z.H. Kafafi, D.B. Chrisey: J. Appl. Phys. **86**, 6451 (1999)
16 Y. Shigesato, D.C. Paine: Appl. Phys. Lett. **62**, 1268 (1993).
17 R.B.H. Tahar, T. Ban, Y. Ohya, Y. Takahashi: J. Appl. Phys. **83**, 2631 (1998)
18 G. Frank, R.L. Kostlin: Appl. Phys. A **27**, 197 (1982)
19 N. Yamada, I. Yasui, Y. Shigesato, H. Li, Y. Ujihira, K. Nomura: Jpn J. Appl. Phys. **38**, 2856 (1999)
20 H. Morikawa, M. Fujita: Thin Solid Films **359**, 61 (2000)
21 E. Gerlach, Rautenberg: Phys. Status Solidi B **86**, 479 (1978)

22 R.B.H. Tahar, T. Ban, Y. Ohya, Y. Takahashi: J. Appl. Phys. **82**, 865 (1997)
23 C. Kittel: *Introduction to Solid State Physics*, 5th edn, Chapt. 6 (Maruzen, Tokyo) 1985
24 C. Erginsoy: Phys. Rev. **79**, 1013 (1950)
25 E. Conwell, V.F. Weiskopf: Phys. Rev. **77**, 388 (1950)
26 R.B. Dingle: Philos. Mag. **46**, 831 (1955)
27 R. Clanget: Appl. Phys. **2**, 247 (1973)
28 A. Fujisawa, T. Nishino, Y. Hamakawa: Jpn. J. Appl. Phys. **27**, 552 (1988)
29 J.R. Bellingham, W.A. Phillips, C.J. Adkins: Thin Solid Films **195**, 23 (1991)